Geologica Acta, Vol.10, Nº 2, June 2012, 85-101
DOI: 10.1344/105.000001744
Available online at www.geologica-acta.com

geologica acta

Microstructural and geochemical analysis of Paleoproterozoic pseudotachylytes in Río de la Plata craton, Tandilia belt, Argentina

M.C. FRISICALE L.V. DIMIERI J.A. DRISTAS V. ARAUJO N. FORTUNATTI

INGEOSUR-CONICET-Departamento de Geología. Universidad Nacional del Sur
San Juan 670. B8000ICN Bahía Blanca, Argentina. Frisicale E-mail: cfrisica@uns.edu.ar. Fax: +54 291 4595148

ABSTRACT

The current study focuses on the analysis of pseudotachylytes from the Azul Megashear Zone, located in the Río de la Plata craton, central Argentina. This shear zone is a strip of mylonitic rocks of more than 40km in length and with a maximum width of 2.5km. Glassy and microcrystalline pseudotachylytes are hosted by Paleoproterozoic gneiss mylonite, granitoid mylonite, granulite mylonite and striped gneisses. The pseudotachylytes occur as fault and injection veins characterized by sharp contacts with no gradation into the mylonites and show melt-origin features such as partially melted quartz and feldspar clasts with embayed rims and flow structures. Their composition is similar to that of the rocks in which they are injected. In those cases involving banded host rocks, slight chemical differences can be observed in the pseudotachylytes mainly in terms of their fabric and mineralogy. Most pseudotachylytes have textures deriving from post-solidification ductile deformation, but others bearing mylonite-like features are related to viscous flow prior to complete solidification. There are indications that some of these pseudotachylytes were formed during the ductile regime, others being generated in the brittle regime during shear zone reactivation following exhumation or uplift. The occurrence of several pseudotachylyte-generating events indicates intermittent aseismic/seismic slip at different crustal levels throughout this shear zone.

KEYWORDS | **Pseudotachylyte. Paleoproterozoic. Río de la Plata craton. Mylonite.**

INTRODUCTION

Pseudotachylyte is a glassy or very fine-grained fault-rock with a very distinct fabric and composed of dark matrix material with minor inclusions of mineral or wall rock clasts (Passchier and Trouw, 2005). Pseudotachylytes can be found in fault zones exhumed by erosion and can be generated either in the brittle regime or in the semi-ductile and ductile regimes. They are frequently associated with cataclastic host rocks (Sibson, 1975; Magloughlin, 1992; O'Hara, 1992; Fabbri *et al*., 2000; Di Toro and Pennacchioni, 2004; Caggianelli *et al*., 2005; Barker, 2005), but have also been reported in connection with mylonitic host rocks (Sibson, 1980; Wenk and Weiss, 1982; Swanson, 1992; McNulty, 1995; Camacho *et al*., 1995; Reynolds *et al*., 1998; Takagi *et al*., 2000; Lin *et al*., 2003). McNulty (1995) reported two types of pseudotachylytes generated at different crustal levels on the Bench Canyon shear zone (Central Sierra Nevada, USA): one generated in the brittle regime associated with uplift or exhumation of the shear zone, and the other generated under the ductile regime, deformed and associated with mylonitic rocks.

The origin of pseudotachylytes has been a subject of discussion for many years, but there is now general agreement that the two main mechanisms of formation are comminution and frictional melting acting simultaneously and with variable intensity during seismic movement along a fault plane (Maddock, 1992; Magloughlin, 1992; Spray, 1992; Wenk *et al.*, 2000; Lin, 2008a; Di Toro *et al.*, 2009).

This paper reports a large pseudotachylyte exposure in a Paleoproterozoic megashear zone in the Río de la Plata craton in Argentina and analyzes the microstructural features and geochemistry of these pseudotachylytes in order to shed light on their possible origin. Their chemical composition in association with host rocks, their interrelationship with mylonitization and the deformation regimes under which they were generated are also discussed.

GEOLOGICAL SETTING

The Río de la Plata craton extends from southern Brazil to Uruguay and Argentina. It is considered a large segment of continental crust mainly formed by successive events of the Transamazonian Orogenic Cycle (Paleoproterozoic) and not significantly affected by the Brasiliano Orogenic Cycle (Neoproterozoic) (Hartmann *et al.*, 2002). The craton is bounded by the Pampean Ranges and the Precordillera on the west and by the Cuchilla de Dionisio (Uruguay) on the east (Fig. 1A). An outstanding feature of the Río de la Plata craton is the absence of deformation events younger than the Mesoproterozoic.

The Tandilia belt system is located in the Río de la Plata craton (Rapela *et al.*, 2007 and references therein). It is composed of a Paleoproterozoic crystalline basement belonging to the Transamazonian cycle and a Neoproterozoic to Lower Paleozoic undeformed sedimentary cover (Fig. 1B). Archean rocks crop out locally. The tectonic evolution of the Tandilia crystalline basement includes several deformation events (Teruggi *et al.*, 1973, 1974; Dalla Salda *et al.*, 1988; Ramos, 1999; Cingolani and Dalla Salda, 2000). U-Pb SHRIMP data for tonalites, trondhjemites, granites and charnockitic gneisses (Hartmann *et al.*, 2002; Cingolani, 2010) suggest that the Tandilia belt was formed between 2234-2065Ma. Rb-Sr and Sm-Nd whole-rock data from the western part of the belt indicate that the parent magmas and granitoid gneisses of the crystalline basement were emplaced in a subduction-

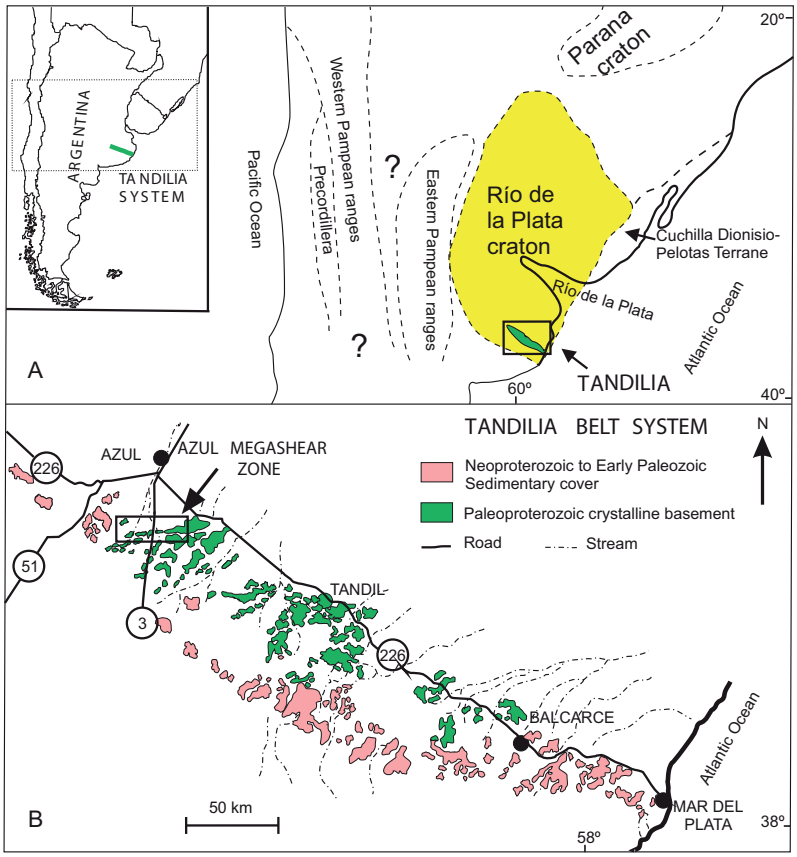

FIGURE 1 | A) Tectonic framework of the Río de la Plata craton. Dashed lines are inferred limits of crustal units (after Rapela *et al.*, 2007). B) Sketch map of the Tandilia System showing major outcrops (after Pankhurst *et al.*, 2003). The square indicates the area of Fig. 2.

related convergent regime 2140±88Ma ago. During the 2200-1700Ma interval, deformation, metamorphism and anatexis occurred with no further contribution to crustal growth by granitoids (Pankhurst *et al*., 2003).

According to Pankhurst *et al*. (2003) deformation related to mylonitization occurred shortly after the granitic intrusion event. The intrusion of undeformed tholeiitic dykes reflects crustal extension related to the later stages of the evolution of the Río de la Plata craton during Mesoproterozoic times (1588±11Ma) (Iacumin *et al*., 2001; Teixeira *et al*., 2001). Since these dykes crosscut the mylonitic zones, the mylonitization is older than the dyke intrusion but younger than the mentioned magmatic event (2140±88Ma).

The pseudotachylytes studied in this paper are located in the Cerro Negro, in the west of the Azul megashear zone, which is part of the northern Tandilia system. This shear zone is a 40km-long belt of mylonitic rocks with a maximum thickness of 2.5kilometers at Boca de la Sierra (Fig. 2A). Early studies define the Azul megashear zone as an E-W-striking, subvertical belt hosted within basement rocks formed mainly by migmatites and rocks of granitic composition (González Bonorino *et al*., 1956; Dalla Salda *et al*., 1981). Protomylonites, mylonites and ultramylonites can be identified. Mylonites and protomylonites predominate and are crosscut by 10-30cm bands of ultramylonites, identifiable by their dark gray color and extremely fine grain (Frisicale *et al*., 2001).

Previous studies on the structural characteristics of the Azul megashear zone (Frisicale *et al*., 2001, 2010) report the most prominent structural elements as being the mylonitic foliation and the presence of mantled porphyroclasts. The mylonitic foliation has a generally vertical orientation in an E-W direction (Fig. 3). In horizontal sections perpendicular to the foliation (XZ), both protomylonites and mylonites have abundant mantled porphyroclasts with well-developed tails of recrystallized grains, symmetric tails being the most common. Asymmetric tails are σ or δ types with opposing shear senses indicating ambiguous movement in the plan-view. In vertical sections normal to the mylonitic foliation (YZ), the occurrence of some porphyroclasts with asymmetric tails indicates a top-to-the-south movement. In sections parallel to the foliation (XY) most porphyroclasts are rounded (Fig. 3). In a few areas the mylonitic foliation exhibits asymmetric folds with subvertical axial planes and subhorizontal axes parallel to the shear zone, indicating vergence towards the south. A notable feature of these rocks is the absence of a marked penetrative mineral lineation.

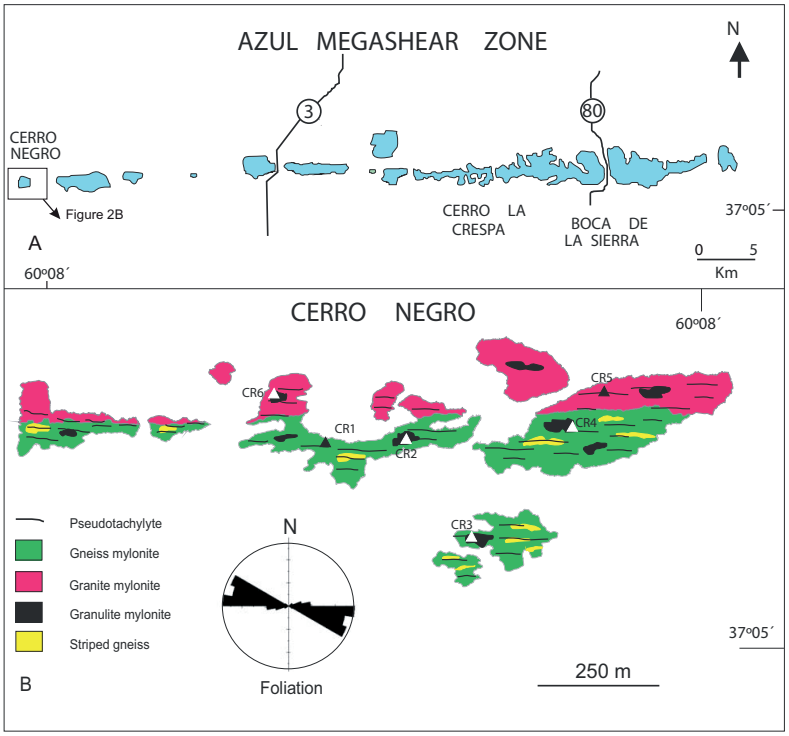

FIGURE 2 | Location of the Cerro Negro pseudotachylytes at the Azul megashear zone within the Tandilia system. A) Simplified geological sketch showing the entire Azul megashear zone comprising rocks of the Buenos Aires complex. B) Geology of the study area showing the bulk distribution of pseudotachylyte veins affecting different rock types, and the location of the study samples: CR1, CR2, CR3, CR4, CR5 and CR6; orientation data of the mylonitic foliation is depicted inside an equal-area projection diagram (lower hemisphere, n: 53).

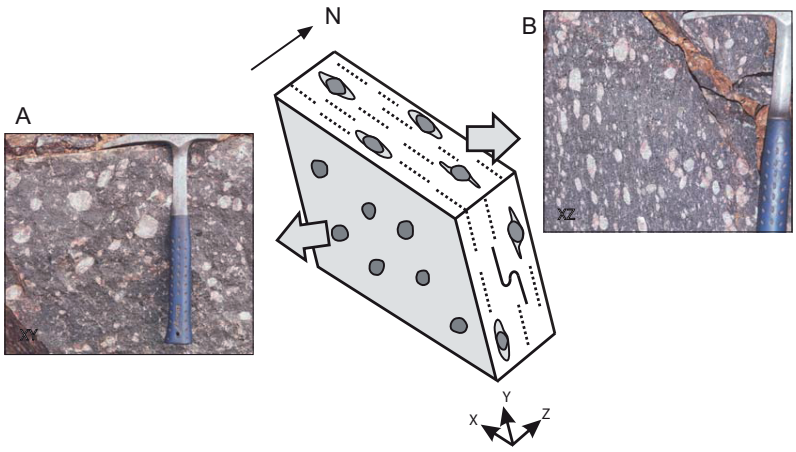

FIGURE 3 | Schematic drawing showing a simplified view of mylonitic foliation and mantled porphyroclasts of Cerro Negro mylonites. A) Photograph of rounded mantled porphyroclasts in the plane of foliation. B) Photograph of mantled porphyroclasts with symmetric or asymmetric tails in a plane normal to the foliation.

On the basis of microstructural analysis of mylonites from different sectors of the Azul megashear zone and the determination of the deformation mechanisms acting on quartz, feldspars, pyroxenes and amphiboles, Frisicale *et al*. (2001, 2004, 2005, 2010) proposed flattening as the main deformation process with a minor transcurrent component. They established that the main dynamic metamorphic event reached the amphibolite facies and locally the granulite facies. Some mylonitic rocks were partially retrograded to greenschist facies.

The kinematics of the Azul megashear zone has not yet been fully elucidated. Some authors (González Bonorino *et al*., 1956; Dalla Salda *et al*., 1981) have interpreted a regional strike-slip faulting with dextral shear sense. More recent studies indicate that shear sense indicators are unreliable since they reflect both dextral and sinistral movements in plan view. These studies support flattening as the main deformation process, suggesting a convergence of the mass rock normal to the Azul megashear zone with subordinate transcurrent movements (Frisicale *et al.,* 1998, 2001, 2005).

The study area (Fig. 2B) at Cerro Negro shows granulite-amphibolite facies mylonites bearing significant amounts of pseudotachylyte and a variety of fault rocks including ultramylonites and rare cataclasites (Frisicale *et al*., 2004, 2006, 2010). Minor exposures of pseudotachylytes occur in other localities of the Azul megashear zone, between Cerro Negro and Cerro de la Crespa hills (Fig. 2A). The suite of fault rocks highlights the development of a shear zone at different crustal levels formed during different times.

HOST ROCKS: MYLONITES

The host rocks of the study area are composed of striped gneisses and mylonitic gneisses, granitoids and granulites with fairly good exposure (Frisicale *et al*., 2006, 2010). Texturally, these mylonites are considered ribbon mylonites according to Passchier and Trouw (2005).

Gneiss mylonite is the most widespread deformed rock in Cerro Negro. Subvertically foliated and medium to coarse-grained, it exhibits compositional banding of quartz-feldspathic and mafic-rich layers, with local ultramylonitic bands 10-20cm wide. At a microscopic level, large fractured orthoclase (<4cm), hornblende (0.01-0.2mm) and plagioclase (0.5mm) porphyroclasts are distributed in a granoblastic matrix composed of quartz, orthoclase, biotite and hornblende. Quartz forms polycrystalline ribbons with an irregular shape. Orthoclase, plagioclase and hornblende porphyroclasts with symmetric or asymmetric recrystallized tails display core-mantle structures of the same composition, in which the core grain is relatively undeformed. Garnet is fractured and locally shows recrystallized tails of finer-grained minerals like biotite and hornblende.

In some parts of the Cerro Negro, gneiss mylonite passes transitionally to striped gneiss (Passchier and Trouw, 2005) with a very thin banding parallel to the regional mylonitic foliation. Sparse orthoclase (2-4mm) and allanite porphyroclasts are disseminated throughout a recrystallized matrix (100-200μm) of orthoclase, opaque minerals and some biotite. Quartz occurs in regular polycrystalline ribbons from 100μm to 500μm wide (Type 3, Boullier and Bouchez, 1978).

Granite mylonites are composed of orthoclase (1-3mm) and garnet (2mm) porphyroclasts in a fine-grained (0.05-0.08mm) quartz-feldspar and minor biotite matrix. Perthitic orthoclase porphyroclasts with symmetric or asymmetric tails display core-mantle structures. The largest crystal face of orthoclase is subnormal to the foliation plane. Strongly fractured garnet porphyroclasts have recrystallized tails. Quartz occurs as polycrystalline ribbons containing subequant grains with straight boundaries.

TABLE 1 Chemical composition of host-rock (CR), bulk pseudotachylyte vein (Pst) and matrix without crystal clasts (M) of Cerro Negro pseudotachylytes. Percentage of pseudotachylyte matrix is: M1 77%, M2 80%, M3 85%, M4 75%

	Gneiss mylonite		Felsic granulite mylonite										Granite mylonite		Mafic granulite mylonite	
Sample	CR 1	Pst 1	M 1	CR 2	Pst 2	M2	CR 3	Pst 3	M3	CR 4	Pst 4	M4	CR 5	Pst 5	CR6	Pst 6
SiO_2	65.98	60.62	60.96	73.45	68.61	68.27	70.72	68.97	67.56	67.01	65.17	64.48	68.69	69.17	57.28	55.66
TiO_2	0.91	1.51	1.54	0.05	0.31	0.33	0.29	0.47	0.54	0.39	0.51	0.59	0.31	0.37	0.83	0.8
Al_2O_3	13.92	13.33	13.56	13.31	14.66	14.84	13.88	14.12	14.85	14.63	15.05	15.14	15.82	15.07	17.12	15.7
Fe_2O_3	5.32	9.45	9.11	1.2	3.71	3.9	2.65	3.54	3.65	4.43	4.66	5.81	3.28	3.41	8.62	9.61
MnO	0.07	0.12	0.11	0.01	0.06	0.06	0.04	0.04	0.04	0.073	0.07	0.09	0.065	0.051	0.143	0.171
MgO	0.87	1.62	1.44	0.08	0.62	0.61	1.08	0.94	1	1.54	1.64	2.02	0.54	0.72	3.26	4.68
CaO	2.55	4.35	4.09	0.85	2.57	2.45	3.19	2.89	3.13	3.62	3.57	3.77	1.88	2.63	6.29	6.95
Na_2O	2.71	2.94	3	2.24	3.22	3.37	2.89	3.21	3.32	2.86	3.4	3.33	2.43	2.88	3.22	3.1
K_2O	6.25	3.75	3.93	7.65	4.69	4.62	3.56	4.2	4.11	4.63	3.72	3.41	5.16	4.43	2.24	2.55
P_2O_5	0.35	0.66	0.8	0.12	0.11	0.33	0.1	0.2	0.23	0.14	0.16	0.21	0.07	0.15	0.3	0.33
LOI	0.56	0.39	0.49	0.7	0.87	0.1	0.83	0.62	0.63	1.22	0.85	0.8	2.54	0.98	0.77	0.88
Total	99.49	98.75	99.01	99.56	99.42	99.39	99.23	99.19	99.06	100.5	98.79	99.63	100.8	99.87	100.1	100.4
H_2O^+	0.93	0.65		0.61	0.7		0.6	0.72								
H_2O^-	0.06	0.33		0.12	0.11		0.03	0.14								

Granulite mylonites are found as blocks or slabs (100-200meters) within the gneiss mylonites and granite mylonites. Taking into account the proportion of pyroxene, they can be classified as felsic granulites (samples 2, 3 and 4, Table 1)and mafic granulites (sample 6, Table 1) (Coutinho *et al.*, 2007). Felsic granulite mylonites are foliated rocks containing weakly elongated feldspar porphyroclasts (orthoclase 40%; plagioclase <5%) as well as elongated hornblende (10%) and orthopyroxene (10%) porphyroclasts in a fine-grained matrix (40%) made up of quartz, orthoclase, plagioclase, hornblende, epidote and opaque minerals. They also exhibit 5-10cm-wide ultramylonite bands. The porphyroclasts are surrounded by polygonal fine-grained rims of the same composition as the core, showing well-developed core-mantle structures formed by grain-size reduction and dynamic recrystallization (Frisicale *et al.*, 2004, 2010). Hornblende porphyroclasts (2mm) have ondulatory extinction and asymmetric shadows composed of fine-grained recrystallized hornblende. Orthopyroxene porphyroclasts, 6mm long, probably hypersthene, are curved and elongated parallel to the mylonitic foliation and contain deformation lamellae parallel to the (100) plane. Narrow ribbons (0.20-0.40mm wide) of fine-grained quartz with straight-grain boundaries perpendicular to the ribbons are parallel to the mylonitic foliation. Texturally, mafic granulite mylonites are similar to felsic granulite mylonites but have a higher proportion of pyroxene (orthopyroxene: 15%, clinopyroxene: 10%), plagioclase (10%) and biotite (10%) and less orthoclase (20%) and hornblende (5%).

PSEUDOTACHYLYTES

Field observations

All mylonitic rocks from the Azul megashear zone, especially those of Cerro Negro, host pseudotachylyte veins. Some veins are found folded at the contact between gneiss mylonite and granite mylonite (Fig. 4A). A number of pseudotachylyte veins show brittle fractures which also affect the host mylonites (Fig. 4B).

Macroscopically, pseudotachylytes are very fine-grained, dark or dark brown with a glassy shine and contain abundant polycrystalline clasts. They occur as fault and injection veins characterized by sharp contacts with the mylonites (Fig. 4B, C); locally contacts tend to be irregular. Fault veins are between 1mm to 20cm thick, the thinner ones being more abundant. Usually fault veins are parallel and separated from one another by a few centimeters. Fault veins are traceable for up to 10m, and over 70% of them are parallel to mylonitic foliation though some veins crosscut it at a low angle (15º-20º) (Fig. 4B, C). Injection veins are perpendicular or oblique to mylonitic foliation and they can connect two fault veins (Fig. 4D).

Microstructure

Thin-sections of Cerro Negro pseudotachylytes are colorless to dark brown, depending on the composition of the host rocks. Pseudotachylytes with a transparent matrix are generated from felsic host rocks such as granite mylonites and striped gneisses. In granulite and gneiss mylonites the higher proportion of mafic minerals darkens the matrix. Pseudotachylytes hosted in granulitic and gneissic mylonites frequently show a symmetrically layered zoning defined by differences in color and matrix-clasts ratio. The margins of most veins are dark and have abundant clasts whereas the central zones are paler and contain more matrix (Fig. 4E). The boundaries between these internal zones are transitional. Pseudotachylytes located along contacts between two different lithologies have clasts of both types of rocks within the vein.

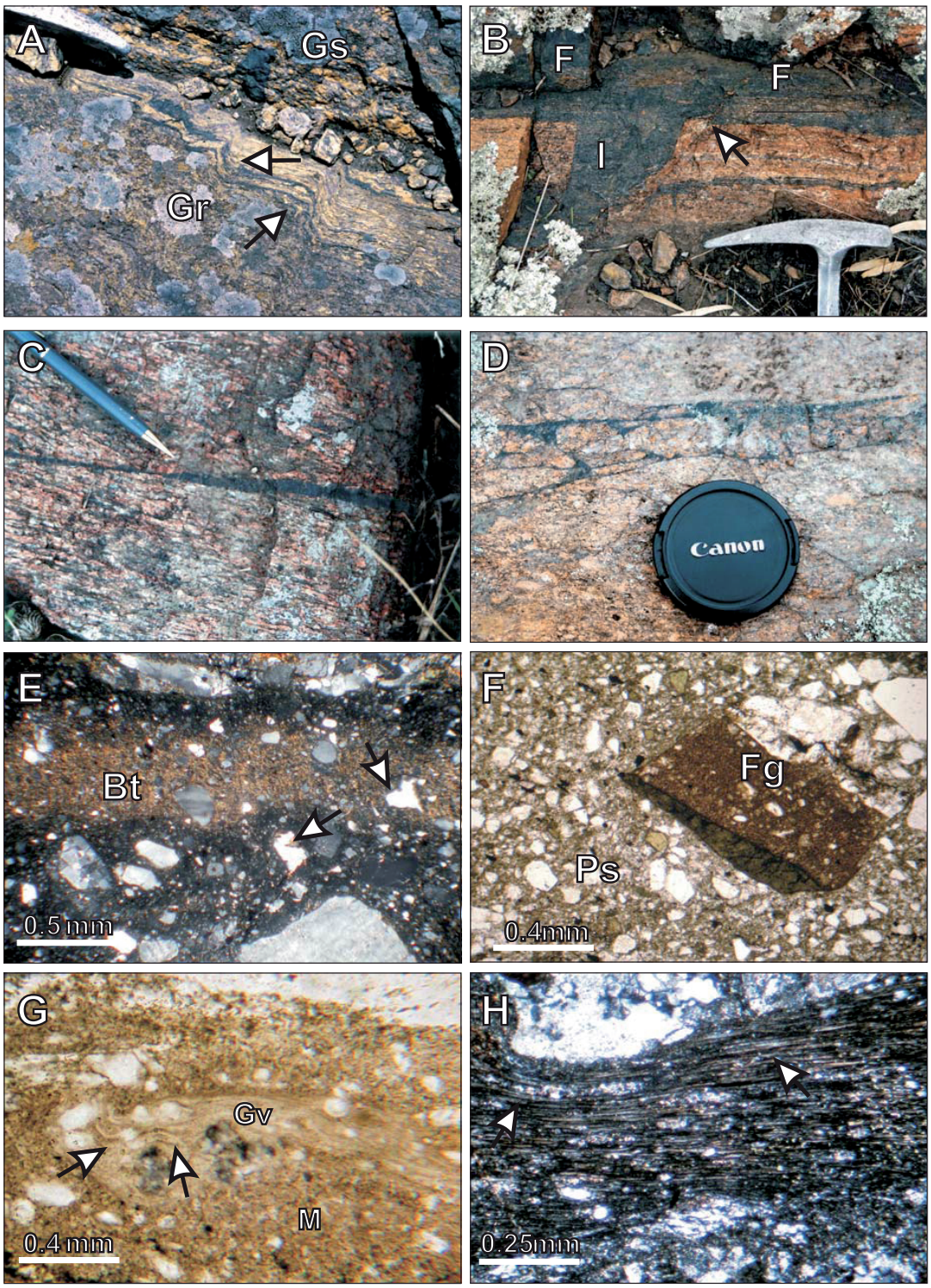

FIGURE 4 | Outcrop photographs A-D) and microphotographs E-H) illustrating structural features of pseudotachylyte veins: A) Two folded fault veins (arrows) injected in the contact between granite mylonite (Gr) and gneiss mylonite (Gs). B) Fault vein (F) and injection vein (I) associated with mylonites; the internal foliation (white line) of the fault vein is parallel to the mylonitic foliation. Brittle fractures affect pseudotachylyte veins and host mylonites (arrow). C) Thin dark pseudotachylyte fault vein cutting the mylonitic foliation at a low angle. D) Network of thin pseudotachylyte veins in a gneiss mylonite. E) Zoned pseudotachylyte vein with rounded and subrounded clasts formed exclusively by quartz and feldspar and a dark microcrystalline groundmass; at the center of the vein, biotite microcrystals (Bt) show a rough alignment in the matrix; some quartz clasts show embayments which evidence partial melting (arrows), F) Pseudotachylyte vein (Ps) with 70/80% of poorly sorted clasts; an older pseudotachylyte fragment (Fg) with sparse clasts is included in a younger pseudotachylyte vein, G) Microcrystalline matrix (M) occupying the marginal zones of a glassy vein (Gv) with flow streaks curved around the clasts (arrows). H) Pseudotachylyte vein with sparse crystal clasts showing thin ribbons parallel to mylonitic foliation (arrows). E) and H) crossed polarized light, F) and G) plane polarized light.

The presence of older pseudotachylyte clasts in younger pseudotachylyte veins (Fig. 4F) and pseudotachylyte veins that cut sharply across old veins are an indication that more than one episode of pseudotachylyte generation took place during the structural evolution of the Azul megashear zone. Similar time relations in pseudotachylytes have been reported elsewhere by Lin (1994, 2008a). Several veins have flow structures with flow streaks roughly parallel to pseudotachylyte boundaries and curved around the clasts (Fig. 4G). Locally, pseudotachylytes show very thin ribbons parallel to the mylonitic foliation of the host rocks (Fig. 4H). This banding is composed of very fine microcrystals of quartz and/or feldspar aligned parallel to the flow streaks. Some pseudotachylyte veins (less than 10%) exhibit planar morphology. Clasts, especially quartz and feldspar, are elongated and flattened parallel to the foliation plane (Fig. 5A, B).

Two types of veins can be distinguished in terms of the proportion of matrix and polycrystalline clasts: veins with more than 80% matrix (Fig. 5A, B, C, D, E) and veins with 70-80% clasts (Fig. 4F). Pseudotachylyte veins with abundant matrix are characterized by quartz and feldspar clasts of diverse shapes and sizes within a fine-grained or glassy matrix. Clasts are generally rounded to sub-rounded and commonly show intense fracturing. The surface of the clasts is often corroded, with rounded and concave borders (Fig. 4E, 5F) indicative of partial melting. Feldspar and quartz clasts often show narrow rims composed of very fine-grained opaque microlites (Fig. 5E). In some cases, these clasts are rotated (Fig. 5F). These veins contain no biotite or hornblende clasts, suggesting that these minerals were entirely melted during pseudotachylyte formation. Garnet from granite mylonites and pyroxene from granulite mylonites, on the other hand, are more resistant to melting and so are commonly found as survivor clasts as they are dehydrated minerals.

Veins with a low proportion of matrix include clasts of quartz, feldspar, pyroxene, hornblende, biotite and garnet. The clasts are angular and their size varies in direct relation to the size of the same minerals in the original host rock and to the fracturing strength of the minerals (Spray, 1992). Biotite, hornblende, garnet and pyroxene have lower resistance to rupture and the corresponding clasts are smaller than quartz and feldspar. Garnet crystals are generally fractured. Small clasts of garnet with a vein-like disposition truncate the contact between pseudotachylytes and the host rocks, suggesting cataclasis and grain-size reduction without significant melt.

Roundness of clasts

The degree of rounding of clasts derived from pseudotachylytes can be used as a quantitative index in understanding the process and mechanism of pseudotachylyte formation (Lin, 1999). A high degree of rounding (>0.4) indicates a melt-origin pseudotachylyte and a lower degree (<0.4) suggests a crushing-origin pseudotachylyte. We analyzed the roundness (Rd) of clasts from four representative samples of Cerro Negro pseudotachylytes by carrying out measurements on photomicrographs of the samples taken under plane polarized light. The selected samples included veins poor in crystal clasts and veins rich in crystal clasts. To reduce measurement errors, clasts larger than 10μm were selected according to Lin (1999). The results were plotted on a roundness-frequency diagram (Fig. 6A) and show that 80% of the clasts have roundness >0.4. Following Lin (1999) this result suggests that the clasts were formed by partial melting of the original crystals rather than cataclasis. Additionally, in order to determine roundness variation across veins in gneiss mylonites, two traverses normal to the contact host rock/pseudotachylyte were made. The traverses crossed two homogeneous pseudotachylytes composed of microcrystalline matrix and clasts of quartz and feldspar. The results were plotted on roundness-traverse diagrams (Fig. 6B) and show only minor variations in clast roundness between the margins and the centre of the veins, indicating that mechanical fragmentation and partial melting affect the whole vein in the same way.

Matrix

The matrix of the Cerro Negro pseudotachylytes has been classified according to Lin (1994) as glass matrix, microcrystalline matrix and mixed matrix. Mixed matrix predominates in most of the veins (55%), followed by microcrystalline matrix (40%) and glass matrix (5%).

Under the microscope, glass matrix is transparent to light brown or yellowish-brown to dark brown, depending on the host rock composition. The matrix is mostly devitrified, very fine-grained, gently anisotropic, with sparse small microcrystals or spherulite microlites visible (Fig. 5E).

Microcrystalline matrix (Fig. 4H; 5C, D) is mainly composed of very fine-grained crystals and small microlites, generally too small to be identified under the optical microscope. The color of the matrix varies from transparent to yellowish-brown or dark brown, depending on the composition. The proportion of microlitic crystals varies widely from very few up to 50%. Microlites are simple or moderately complex in morphology and can be acicular, granular, lath-like, spherulitic or globular. In a transparent matrix (Fig. 5D), globular microlites consist of quartz-feldspar intergrowths probably resulting from the rapid growth from a melt (Lin, 1994, 2003). In colored matrix (Fig. 5A, B, C, F), microlites show slight pleochroism and straight extinction and have an acicular, lath-like shape,

usually aligned, probably formed by direct crystallization from the melt (Lin, 2008a). X-ray diffraction data obtained from the colored matrix indicate that it is formed by biotite. Very fine-grained opaque granular microlites and spherulite microlites are observed in some of these veins (Fig. 5C, E). Detailed analyses of two pseudotachylytes with a microcrystalline matrix were carried out with a LEO 40-XVP scanning electron microscope: one has a relatively porous matrix with a fine equigranular texture (<1μm), glassy fragments, conchoidal fracture and sparse vesicles (Fig. 7A) and with some of the microlites showing a typical polyhedral shape (Fig. 7B). The other has a microcrystalline matrix characterized by a strong preferred orientation and is composed of very fine grains

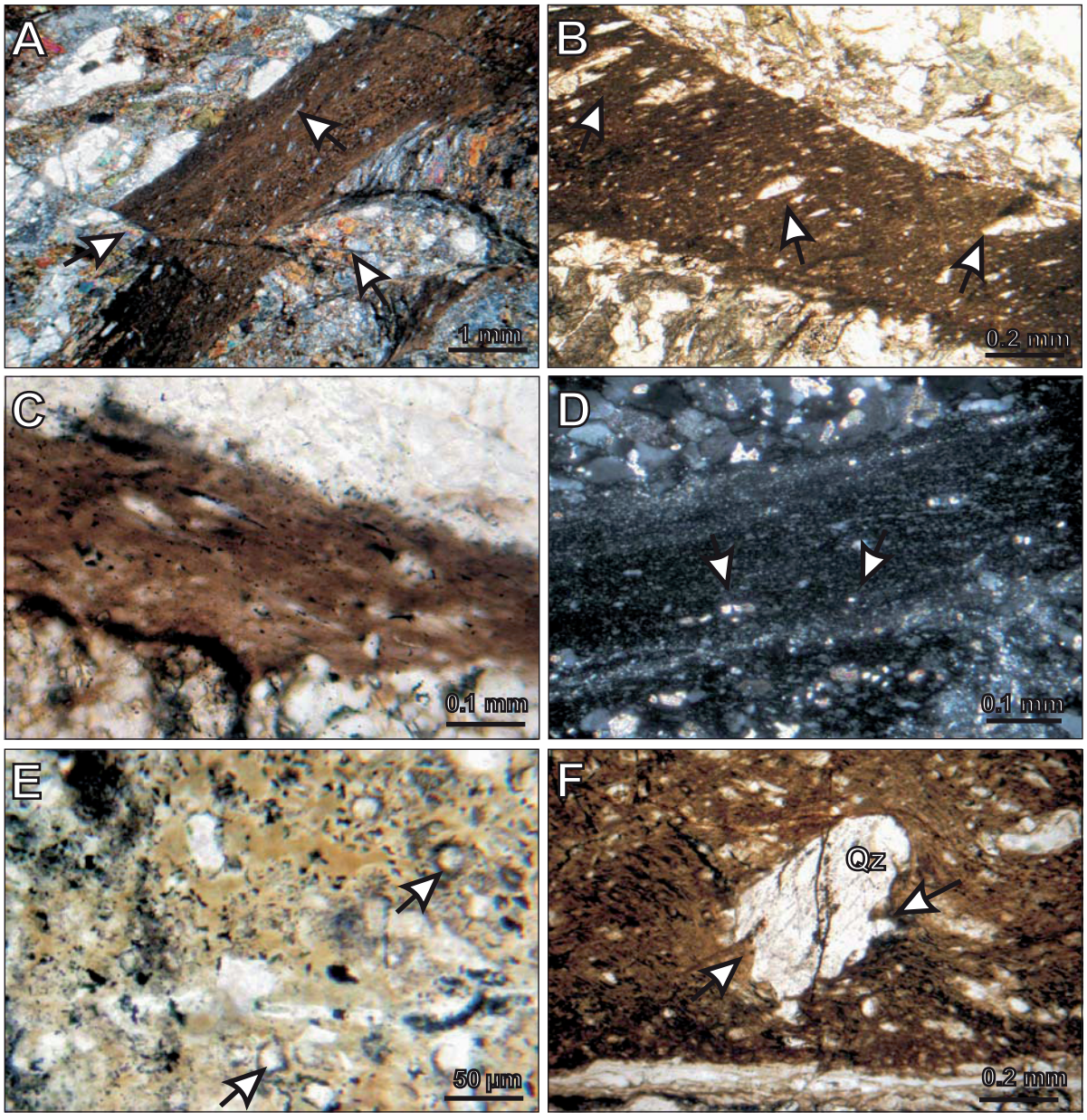

FIGURE 5 | Photomicrographs showing microstructural characteristics of pseudotachylytes. All photomicrographs are in plane polarized light, except A) and C), which are in crossed polarized light. A) Crystal clasts flattened parallel to the mylonitic foliation; the pseudotachylyte vein is broken and displaced by a later brittle fracture (arrows). B) Detail of (A) showing flattened quartz clasts (arrows) and the preferred orientation of clasts within the vein. C) Microcrystalline matrix, probably formed by fine biotite microcrystals; opaque minerals form tiny pressure shadows in crystal clasts (arrows). D) Pseudotachylyte vein with microcrystalline matrix. E) Glassy matrix with very fine-grained microlites of opaque minerals; feldspar and quartz clasts have narrow rims composed of opaque microlites (arrows), plane polarized light. F) Sheared quartz porphyroclast (Qz) with embayments (white arrows) suggesting partial melting before mylonitic ductile deformation.

with rounded borders which bear vesicles and hourglass-shaped strings (Fig. 7C). The particularity of the strings' appearance comes from the glassy material that bridges crack gaps between melted grains (Spray, 1992; Otsuki *et al*., 2009). In some cases the microcrystalline matrix has aligned biotite microcrystals (Fig. 7D).

Mixed matrix is typically anisotropic in thin section, and locally variable in color from colorless to brown or yellowish-brown under the optical microscope. It is composed of a combination of microlites and glassy material and shows similar textural features to those of the microcrystalline and glassy matrix. Glassy material is mostly devitrified and the microlites show a variety of shapes: acicular, granular, lath-like, spherulitic and globular. Usually this matrix is quite homogeneous but may contain a compositional layering which follows the contours of the veins. In these cases, the microcrystalline matrix occupies the marginal zones of glassy veins (Fig. 4G).

GEOCHEMISTRY

The bulk chemical compositions of pseudotachylyte veins (including clasts), pseudotachylyte matrix and related country rocks were measured by fusion Inductively Coupled Plasma-Mass Spectrometry (ICP-MS) at Activation Laboratories Ltd. (ACTLABS), Canada. Crystalline water (H_2O^+) and pore (fractured) water (H_2O^-) of six samples (host rocks and pseudotachylyte veins) were analyzed independently by gravimetry. The results of the chemical analysis are shown in Table 1. The An-Ab-Or classification diagram based on normative feldspar composition shows that host rocks have granitic and granodioritic composition (Fig. 8A). Figure 8B illustrates the relationship between host rocks and pseudotachylyte matrix normative composition. Bulk pseudotachylytes (clasts+matrix) show a cluster of similar normative feldspar composition close to the granite minimum melt composition (Chen and Grapes, 2007). Bulk pseudotachylytes are richer in normative plagioclase than the host rock and have a lower proportion of normative orthoclase, with the exception of one felsic granulite mylonite (CR3-Pst3) and the mafic granulite mylonite. These two latter pseudotachylytes have relatively more normative orthoclase than plagioclase (Fig. 8B), which is consistent with a slight enrichment in K_2O relative to the host granulites and can be partially attributed to preferential melting of orthoclase over plagioclase in the host rocks (Fig. 9, 10).

The composition of the pseudotachylyte matrix was analyzed using four samples with clasts greater than 0.5mm. The clasts were handpicked under a stereo microscope to separate them from the matrix. The average bulk composition of pseudotachylyte veins (clasts+matrix: Pst), matrix (M) and associated host rocks (CR) shows moderate correspondence among all samples (Fig. 9). Bulk pseudotachylytes and matrix have lower SiO_2 and K_2O content and higher Fe_2O_3, MgO, Na_2O, CaO and TiO_2 content than the host rock. The chemical differences between gneiss mylonite (CR1) and felsic granulite mylonites (CR2 and CR3) and bulk pseudotachylytes are more pronounced, indicating preferential melting of amphibole and biotite rather than quartz and feldspar. Felsic granulite mylonite (CR4), granite mylonite (CR5) and mafic granulite mylonite (CR6) show minor

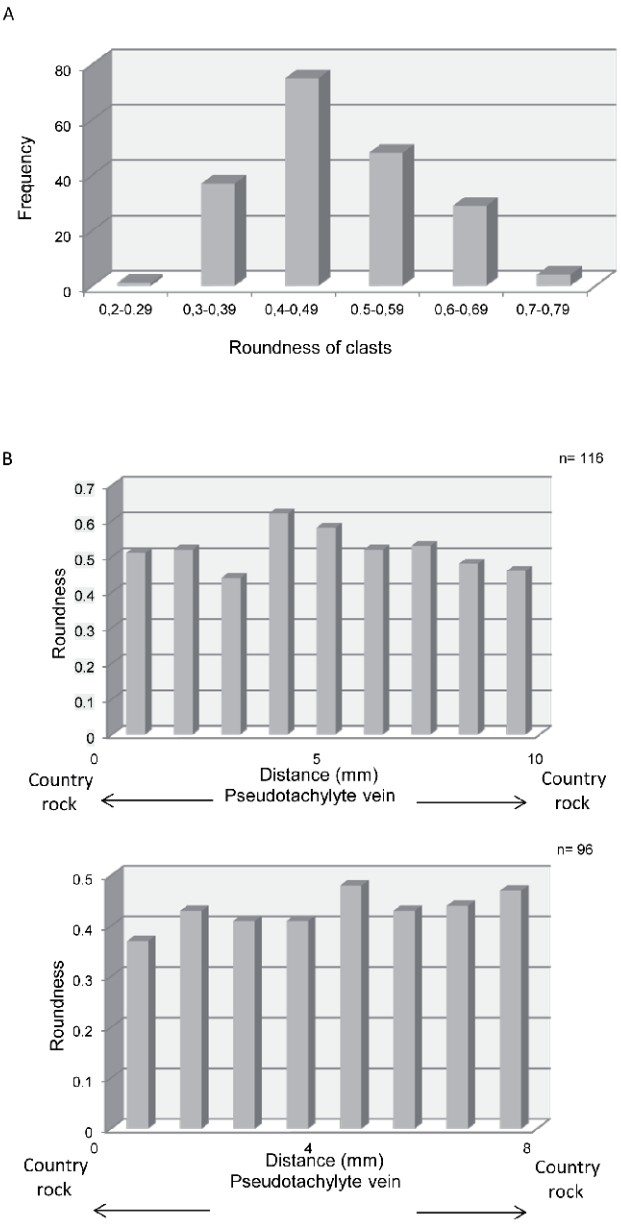

FIGURE 6 | Roundness frequency diagram of clasts of Cerro Negro pseudotachylytes, N: number of measurements. A) Melt-originated pseudotachylytes. B) Roundness-traverse diagrams showing two traverses normal to the country rock/pseudotachylyte contact.

chemical disparity with respect to their corresponding pseudotachylytes. Pseudotachylyte samples Pst1-M1 and Pst2-M2 differ significantly from the host rocks but show only minor variations with their corresponding matrix, indicating no differentiation. Pseudotachylytes Pst3 and Pst4, on the other hand, show some differences with respect to their matrix (M3 and M4). Pseudotachylyte matrix has lower SiO_2, K_2O and Na_2O content and higher Fe_2O_3, MgO and CaO content than bulk pseudotachylytes as a consequence of selective melting giving rise to the preferential assimilation of the ferromagnesian phases and perthitic orthoclase rather than plagioclase (Spray, 1992).

Most pseudotachylytes and host rocks have quite similar LOI values (loss on ignition) and water content (H_2O^+ and H_2O^-) (Table 1). The crystalline water content represents the initial water dissolved in the melt associated with the quenching of the melt (Lin, 2008b). The low crystalline water (H_2O^+) content in these samples and the scarcity of vesicles and amygdales indicate that melting could have occurred under dry conditions. The different LOI values obtained for sample CR5 (granite mylonite) can be attributed to the presence of secondary minerals like calcite and epidote, crystallized particularly at the contact between pseudotachylyte veins and host rock, indicating considerable fluid flux after pseudotachylyte formation.

The major element composition of the different host rocks and pseudotachylytes was plotted in an isocon diagram (Grant, 1986) (Fig. 10) to investigate the possibility of preferential melting of specific mineral phases. Melting was assumed to occur at constant mass. Figure 10 shows that oxides display different mobility during melting. The enrichment in Fe_2O_3, MgO, TiO_2 (Pst1, Pst2, Pst3) and CaO (Pst1, Pst2), and depletion of SiO_2 compared to the host rock (Fig. 10A, B, C), is attributed to preferential melting of biotite (CR1, CR2, CR3) and hornblende (CR1, CR2). The behavior of

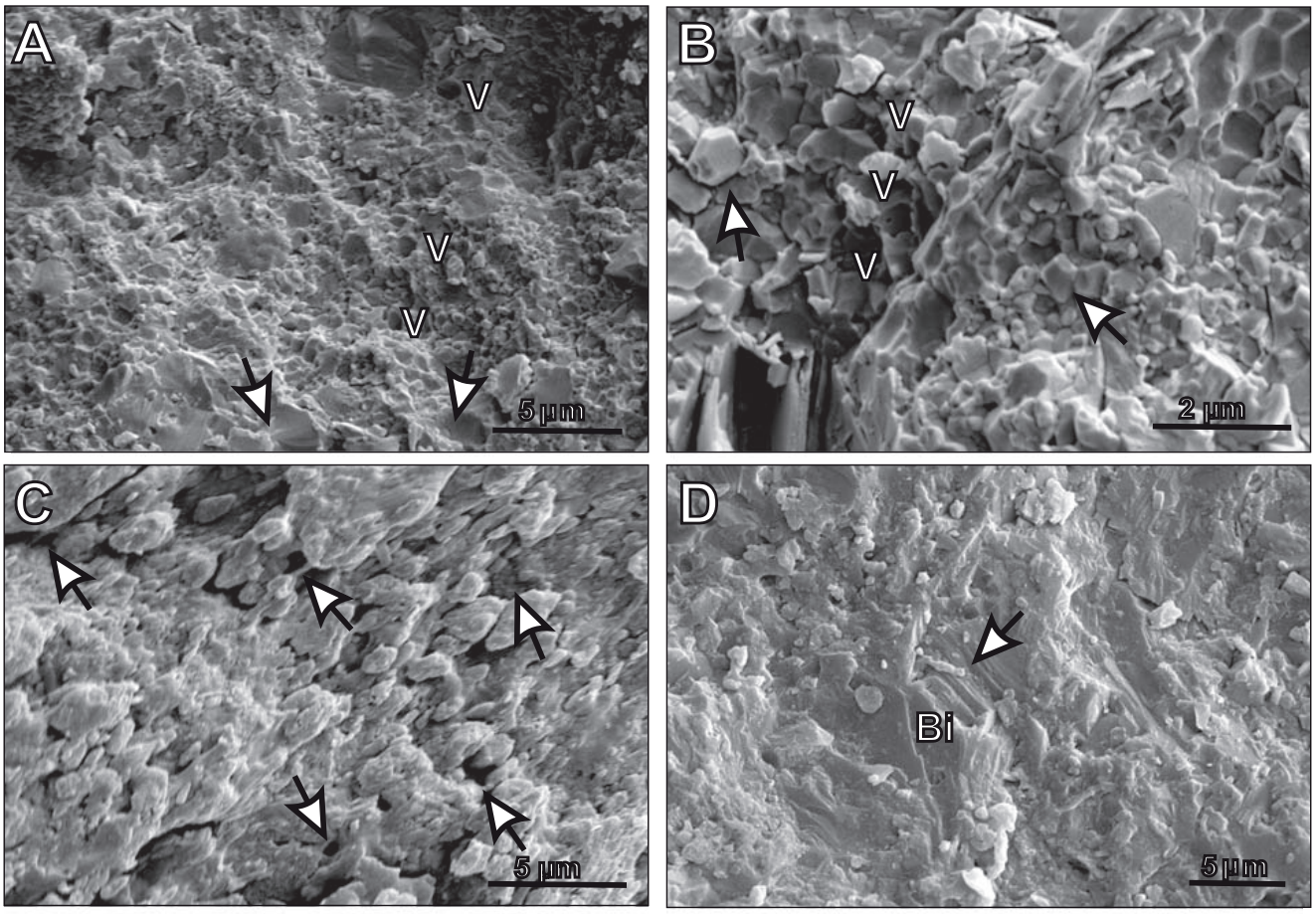

FIGURE 7 | SEM image of typically ruptured surface texture of Cerro Negro pseudotachylytes. A) Textures of pseudotachylyte veins with microcrystalline matrix mixed with sparse clasts, glass with conchoidal fractures (arrow) and vesicles (V). B) Microcrystalline matrix with equigranular and polyhedral texture (arrow) and well-developed vesicles (V). C) The surface shows gruel-like texture with hourglass-shaped springs of melt materials (white arrow), and vesicles (black arrow). D) Micron-sized biotite flakes interpreted as microlites quenched from rapidly cooling melt; note the alignment of biotite microlites (Bi).

Na_2O, K_2O and CaO is associated with variable melting of plagioclase relative to orthoclase. The compositions of host rock and corresponding pseudotachylytes of samples CR4-Pst4, CR5-Pst5 and CR6-Pst6 are quite similar (Fig. 10D, E, F; Table 1). This is consistent with near total melting of the host rock (O'Hara and Sharp, 2001; Lin, 2008a). The slight enrichment in CaO and Na_2O and depletion in K_2O in Pst5 suggests limited preferential melting of plagioclase over orthoclase. The loss of LOI (Fig. 10E) is related to fluid flux after pseudotachylyte formation. This component behavior is associated with the melting processes (whether preferential or complete melting) and with the textural heterogeneity of the host rocks.

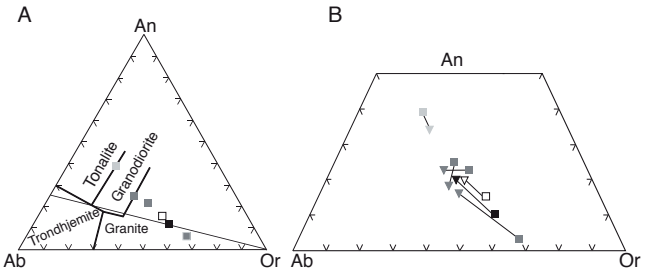

FIGURE 8 | A) Classification of granitic rocks according to their normative Ab-An-Or composition after Barker (1979) (heavy lines) for country rocks. B) An-Ab-Or normative diagrams showing the evolution of feldspar compositions from host rocks to pseudotachylyte veins, connected by tie lines.

DISCUSSION

Processes of pseudotachylyzation: melting versus crushing

The microstructures of the pseudotachylytes injected in Cerro Negro mylonites indicate that most of them were generated by frictional melting (Fig. 6A, B). A melt origin for these pseudotachylytes is supported by the following features:

1) quartz and feldspar with rounded shapes and embayed rims;
2) sparse biotite and hornblende clasts, reflecting the preferential destruction and assimilation of these minerals during melting;
3) veins with flow structures parallel to the edges and curved around the clasts;
4) the occurrence of new crystallized microlites (*i.e.* biotite) and spherulites;
5) hourglass-shaped springs between grains.

Likewise, the roundness of quartz and feldspar clasts (>0.4) confirms that they derived from frictional melting of the country rocks rather than crushing (Lin, 1999). Other Cerro Negro pseudotachylyte veins with sparse matrix and abundant angular clasts could indicate that comminution predominates over frictional melting.

Host rock-pseudotachylyte compositional variations

A distinctive characteristic of some pseudotachylytes injected in Cerro Negro mylonitic rocks is that their chemical composition (matrix plus clasts) does not differ significantly from the chemical composition of the host rock, a common feature reported elsewhere by Sibson (1975); Magloughlin (1992); Maddock (1992); Spray (1992); Lin (1994, 2008a); Camacho *et al*. (1995); Di Toro and Pennacchioni (2004); Di Toro *et al*. (2009). This characteristic is clearly depicted in the isocon diagram (Fig. 10). However, samples CR2 and to a lesser extent CR1 and CR3 have some compositional differences. Maddock (1992) reported that the chemistry of pseudotachylytes depends on the composition, mineralogy and fabric of the host rock. This author suggests that pseudotachylyte composition in gneissic rocks is defined by the rapid preferential breakdown of hydrated ferromagnesian minerals relative to felsic minerals due to cataclasis and melting processes. This process is also reported by Thompson and Spray (1996) for Sudbury pseudotachylytes. Warr *et al*. (2003) observed compositional variations in pseudotachylyte friction melts and attributed them to crystal fractionation of the melt during transport.

Preferential melting occurs in those Cerro Negro host rocks characterized by a strong compositional banding, like gneiss mylonite (CR1) and felsic granulite mylonites (CR2, CR3). Homogeneous Cerro Negro rocks with poor compositional banding, as felsic and mafic granulite mylonites (CR4, CR6) and granite mylonite (CR5), display compositional similarities with their hosted pseudotachylytes, especially in concordant fault veins (Maddock, 1992). The slight compositional differences with pseudotachylytes (Fig. 10A, B, C) can therefore be explained by the nature of the fabric and the mineralogy of Cerro Negro host rocks.

The water content of Cerro Negro pseudotachylytes and host rocks is quite similar (Table 1), indicating low water activity during the generation of the pseudotachylytes. According to Caggianelli *et al*. (2005) the existence of biotite microlites in pseudotachylytes indicates that they formed in the presence of water. Since biotite and hornblende are present in host rocks in the Azul megashear zone, biotite microlites could be formed by crystallization from the melt or recrystallization from the glass fraction.

Equilibrium and non-equilibrium melting

Cerro Negro pseudotachylyte veins generally contain few ferromagnesian mineral clasts like biotite and hornblende, and the SiO_2 content of the matrix is lower than that of host gneiss and felsic granulite mylonites (Table 1). This indicates a selective non-equilibrium melting of wall-rock. Generally, pseudotachylyte melts are more mafic in composition than the host rock because of the preferential melting of mafic minerals. This is the strongest indication that disequilibrium melting, rather than eutectic melting, took place during pseudotachylyte generation (Maddock, 1992; Lin, 1994, 2008a; Lin and Shimamoto, 1998). Spray (1992) points out that melting is a selective process where the ferromagnesian phases making up the host rock are preferentially assimilated. This author proposes that frictional melting depends directly on the mineral constituents and that the occurrence of hydrated minerals considerably increases the probability of producing melting during a co-seismic event. In the case of pseudotachylytes injected in granite (CR5) and in granulite mylonites (CR4, CR6), which have little or no biotite and hornblende, the SiO_2 content of the matrix is almost identical to the whole rock (Table 1), suggesting that in these rocks melting is close to equilibrium.

Evolution of pseudotachylytes in a mylonite zone

The pseudotachylytes of Cerro Negro originated under different tectono-metamorphic conditions during the evolution of the Azul megashear zone, going through ductile to fragile regimes. They were formed by comminution and friction-induced melting along a fault surface during seismic slip as described by McKenzie and Brune (1972); Sibson (1975); Spray (1995); Lin (2008a, b); Di Toro *et al.* (2009). Although many pseudotachylytes throughout the world are commonly associated with cataclasites (Magloughlin, 1992; Fabbri *et al.*, 2000; Lin, 2008a; Di Toro *et al.*, 2009), Cerro Negro pseudotachylytes are mainly related to mylonites and display an overprinted ductile deformation. Studies in other regions have also reported that pseudotachylytes are formed by seismic faulting within a ductile-dominated regime showing a superposed ductile deformation (McNulty, 1995; Camacho *et al.*, 1995; Reynolds *et al.*, 1998; Lin *et al.*, 2005; Lin, 2008a; Di Toro *et al.*, 2009).

Several pieces of evidence point to the formation of some Cerro Negro pseudotachylytes during a ductile regime; for example, fault veins that show internal foliation parallel to the mylonitic foliation of the host rock indicate that such veins were mylonitized during subsequent ductile deformation (Fig. 4B). Additionally, folding of the mylonitic foliation together with interlayered fault veins (Fig. 4A) and foliated veins with fine band-like ribbons parallel to the mylonitic foliation (Fig. 4H) are indicative of plastic deformation. The presence of elongated and flattened clasts, in particular quartz and feldspar (Fig. 5A, B) and rotated porphyroclasts (Fig. 5F), indicates plastic deformation of the

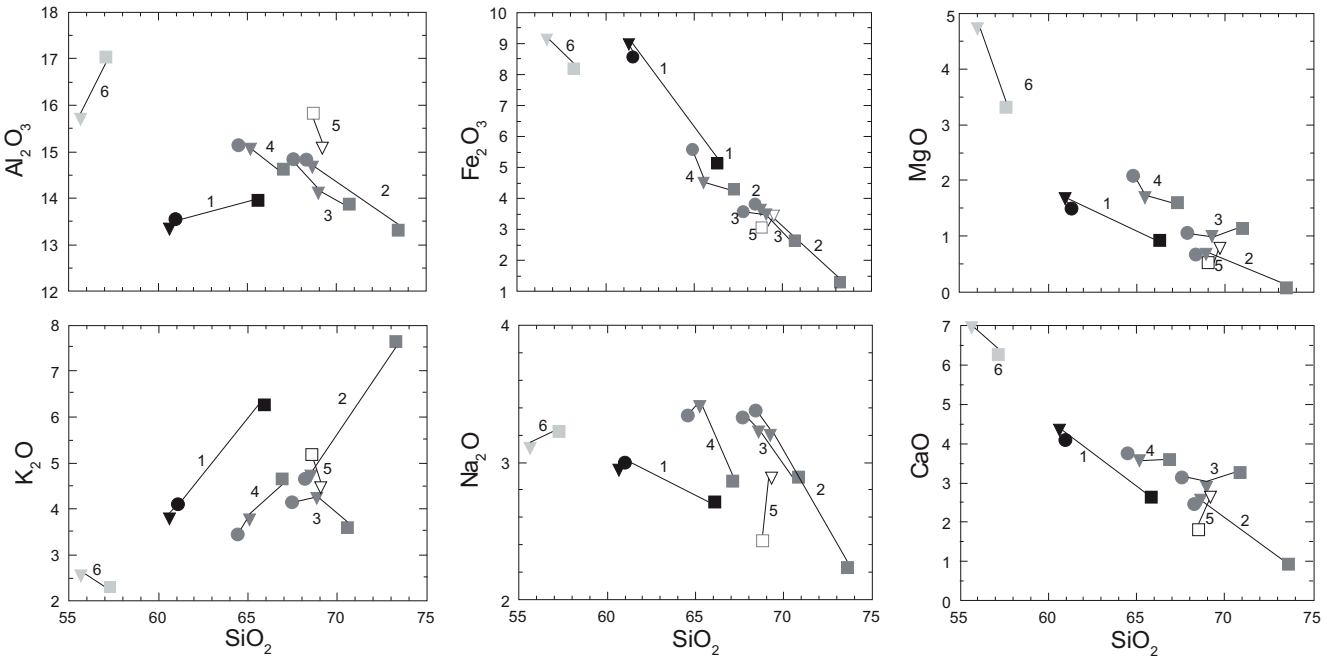

FIGURE 9 | Variation diagrams showing changes in major element concentration in pseudotachylytes (triangles) and matrix (circle) compared to their host rocks (squares), connected by tie-lines. Numbers represent samples (1: CR1-Pst1-M1). Weight percent oxides.

fragments and reorientation parallel to the mylonitic foliation subsequent to pseudotachylyte formation. The biotite microlite alignment observed in the microcrystalline matrix of Cerro Negro (Fig. 5C) can be attributed to ductile behavior as reported by McNulty (1995) for pseudotachylytes of the Bench Canyon shear zone.

There is also evidence showing that some Cerro Negro pseudotachylytes were generated under a brittle regime associated with shear zone reactivation during exhumation or uplift. This is supported by the presence of abundant irregular pseudotachylyte fault and injection veins intruding connected fractures, forming a web-like network and generally crosscutting the mylonitic foliation (Fig. 4C, D). Furthermore, the existence of older pseudotachylyte fragments in younger pseudotachylyte veins suggests that the former were broken before the new pseudotachylyte reworks included them (Fig. 4F).

The texture of most Cerro Negro pseudotachylytes derives from post-solidification ductile deformation, though pseudotachylytes with mylonite-like features are related to viscous flow before complete solidification (Fig. 4G) and share the same characteristics as pseudotachylytes originating in the brittle regime or in the brittle-ductile transition (Fig. 4E, F, G). It is likely that most of the textural features produced by melt flow are completely overprinted by mylonitization of pseudotachylytes formed in a ductile-dominated regime.

The coexistence in the same fault zone of pseudotachylyte veins originating in ductile-to-brittle regimes indicates that they were generated by repeated seismic slip during rapid exhumation of a collisional zone as illustrated by Lin *et al*. (2003). In addition, Di Toro *et al*. (2009) point out the existence of pseudotachylytes associated with mylonites at greenschist, amphibolite and granulite facies.

Briefly, Cerro Negro pseudotachylyte veins were formed at different depths from ductile-dominated to brittle-dominated regimes. We identified several pseudotachylyte-generating events in a ductile-dominated

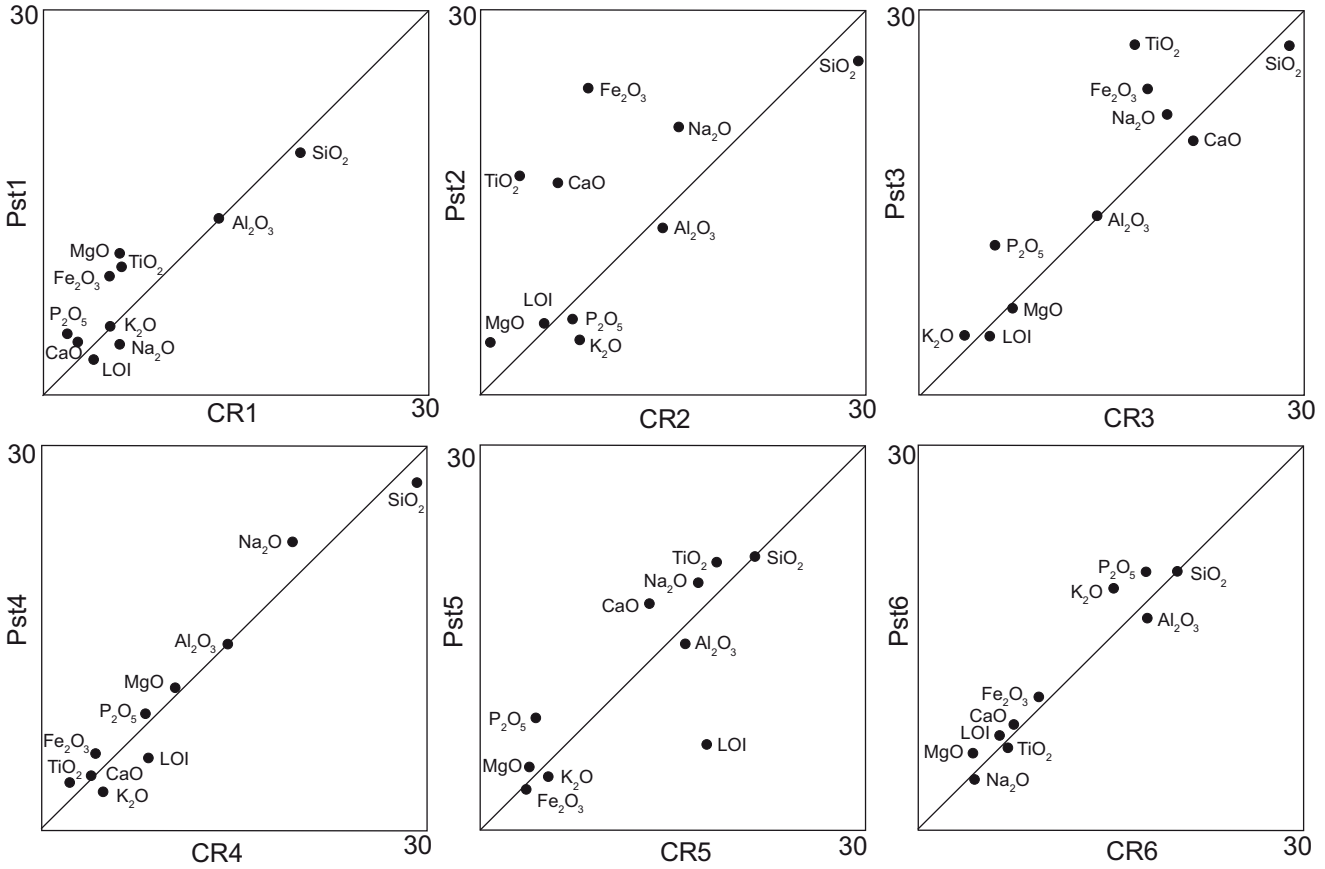

FIGURE 10 | Isocon diagrams of chemical compositions of Cerro Negro pseudotachylytes and their country rocks, according to Geoiso, a program that enables the calculation of mass balances in geologic processes (Coelho, 2005). Al_2O_3, Na_2O and LOI are considered immobile elements during comminution and frictional melting of the country rocks and lie on or close to a straight line through the origin (isocon). Elements plotting above the isocon represent relative gains, while those below the isocon represent relative losses.

regime. The resulting pseudotachylytes were mylonitized during subsequent ductile deformation. The mylonitic foliation and older pseudotachylytes were subsequently overprinted by younger pseudotachylyte veins during uplift and exhumation of the shear zone into the brittle region.

Deformation regime and PT path of pseudotachylytes

The metamorphic conditions under which these pseudotachylytes were formed coexisted temporally with mylonites in the same fault zone, indicating that they originated under similar P-T conditions. Deformation temperatures calculated using Thermocalc (Powell *et al*., 1998) for mylonites in the central sector of the Azul megashear zone (Boca de la Sierra, Fig. 2), together with microstructural data, suggest that mylonitization occurred in the range of 400° to 450°C and pressures above 600MPa, indicative of greenschist to amphibolite facies conditions (Frisicale *et al*., 2005). At the western end of the Azul megashear zone (Cerro Negro, Fig. 2), the analysis of deformation mechanisms of quartz, feldspar, amphibole and pyroxene of mylonites indicates that deformation occurred under higher metamorphic conditions, reaching upper amphibolite to granulite facies (Frisicale *et al*., 2010). Cerro Negro mylonites show evidence of dynamic recrystallization of orthoclase and plagioclase, and granoblastic microstructures in plagioclase and amphibole (Frisicale *et al*., 2010). These features show that deformation in this region occurred at temperatures above 500°C with the amphibolite facies as a lower limit as suggested elsewhere by Pryer (1993) and Trouw *et al*. (2010). Likewise, the presence of orthopyroxene deformed by intracrystalline processes in these mylonites (Frisicale *et al*., 2010) suggests metamorphic conditions from medium to high grade (Brodie, 1998; Passchier and Trouw, 2005; Trouw *et al*., 2010), with pressure reaching up to 900MPa (Kruse and Stünitz, 1999). Furthermore, the presence of striped gneiss and ribbon mylonites in Cerro Negro indicates that deformation would have occurred under high-grade metamorphism, with temperatures above 650°C (Passchier and Trouw, 2005; Trouw *et al*., 2010).

In order to establish a sequence of pseudotachylyte development, a schematic diagram was devised (Fig. 11) depicting three possible paths for the injection of Cerro Negro pseudotachylyte veins during ductile to brittle regimes. The paths show the main processes responsible for the generation of a pseudotachylyte according to Maddock (1992). The older generation of Cerro Negro pseudotachylytes is likely to have formed under the conditions marked by path 1 (Fig. 11) since the estimated peak temperature of mylonitization ranged between 600º and 700ºC and the pressure between 600 and 900MPa (Frisicale *et al*., 2005, 2010). This path represents the evolution of Cerro Negro pseudotachylytes formed in a

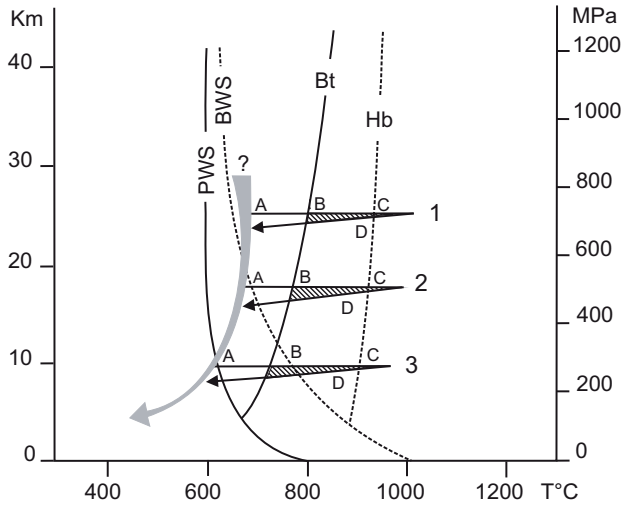

FIGURE 12 | Schematic diagram illustrating repeated pseudotachylyte generation in the same fault zone through time and different crustal levels. The estimated conditions of metamorphism and melt generation for Cerro Negro pseudotachylytes together with selected melting reactions are indicated. PWS: pelite wet solidus; BWS: basalt wet solidus; Bt: biotite dehydration melting curve; Hb: hornblende dehydration melting curve, (all curves after Chen and Grapes, 2007). Peak metamorphic conditions of mylonitization are estimated between 600-700ºC and 800MPa. Grey arrow represents the probable path of the Cerro Negro shear zone during uplift or exhumation. Along the indicated paths (1, 2, 3), initial fracturing and comminution occurs in (A). The first melt (B) formed when temperature crossed the dehydration- melting biotite solidus (Bt). (C) Indicates beginning of hornblende dehydration-melting; in (D) freezing and crystallization of the melt (Maddock, 1992).

ductile regime. Path 2 corresponds to a subsequent event of pseudotachylyte generation produced during uplift of the megashear zone and dominated by conditions of a fragile-ductile transitional environment. Path 3 would be followed by the younger pseudotachylytes, closely associated with brittle deformation.

CONCLUSIONS

This study provides new evidence of the existence of intermittent aseismic/seismic slip within the development of the Azul megashear zone at different crustal levels. The Azul megashear zone is a large Paleoproterozoic mylonite zone formed under amphibolite and granulite facies conditions within the Tandilia belt. Many of the numerous pseudotachylyte veins occurring in the west of this mylonitic zone at Cerro Negro have textural characteristics indicating a ductile regime origin.

The presence of rounded clasts, embayed rims, flow structures, new crystallized microlites and hourglass-shaped springs of melt material suggest predominant frictional melting rather than crushing for the formation of most pseudotachylytes. In addition, the bulk chemical composition of pseudotachylytes (matrix plus clasts)

and host rocks is similar, suggesting total melting of the host rocks. Slight chemical differences observed in pseudotachylytes hosted in banded rocks can be explained by the nature of their fabric and mineralogy.

Some pseudotachylyte veins with few ferromagnesian mineral clasts and with lower SiO_2 content than their host gneiss and felsic granulite mylonites are indicative of a selective non-equilibrium melting of wall-rock.

Seismic faulting occurred repeatedly in the Cerro Negro region under both ductile and brittle regimes, generating different events of pseudotachylyte formation. This process gave birth to older pseudotachylytes that were subsequently overprinted by mylonitization during aseismic deformation and to younger pseudotachylytes associated with cataclastic deformation during uplift and exhumation of the shear zone. These younger pseudotachylytes crosscut older pseudotachylytes and the mylonitic foliation.

ACKNOWLEDGMENTS

The authors sincerely thank A. García Casco and Montserrat Liesa for their careful review of previous versions of the paper and for their many suggestions for improvement. The authors are also grateful to Drs. A. Lin and O. Fabbri for their constructive reviews which greatly enhanced the manuscript. This research was supported by grants to the authors from Universidad Nacional del Sur, CONICET and Agencia Nacional de Promoción Científica y Tecnológica. The Department of Geology and INGEOSUR of Universidad Nacional del Sur are gratefully acknowledged.

REFERENCES

Barker, S.L., 2005. Pseudotachylyte-generating faults in Central Otago, New Zealand. Tectonophysics, 397, 211-223.

Boullier, A.M., Bouchez, J.L., 1978. Le quartz en rubans dans les mylonites. Bulletin of the Geological Society France, 20, 253-262.

Brodie, K., 1998. High-temperature mylonites: I. Metabasic mylonites. In: Snoke, A., Tullis, J., Todd, V. (eds.). Fault-related rocks. A Photographic Atlas. Princeton, Princeton University Press, 428-435.

Caggianelli, A., de Lorenzo, S., Prosser, G., 2005. Modelling the heat pulses generated on a fault plane during coseismic slip: Interferences from the pseudotachylytes of the Copanello cliffs (Calabria, Italy). Tectonophysics, 405, 99-119.

Camacho, A., Vernon, R.H., FitzGerald, J.D., 1995. Large volumes of anhydrous pseudotachylyte in the Woodroffe Thrust, eastern Musgrave Ranges, Australia. Journal of Structural Geology, 17(3), 371-383.

Chen, G.N., Grapes, R., 2007. Granite genesis: In-situ melting and crustal evolution. Dordrecht (The Netherlands), Springer, 277pp.

Cingolani, C.A., 2010. The Tandilia System of Argentina as a southern extension of the Río de la Plata craton: an overview. International Journal of Earth Sciences, 100(2-3), 221-242.

Cingolani, C.A., Dalla Salda, L.H., 2000. Buenos Aires cratonic region. In: Cordani, U., Milani, E., Thomaz Filho, A., Campos, D. (eds.). Tectonic evolution of South America, Rio de Janeiro, Brazil, 139-146.

Coelho, J., 2005. GEOISO-A WindowsTM program to calculate and plot mass balances and volume changes occurring in a wide variety of geologic processes. Computers & Geosciences, 32, 1523-1528.

Coutinho, J., Kräutner, H., Sassi, F., Schmid, R., Sen S., 2007. Amphibolite and Granulite. In: Fettes, D., Desmons, J. (eds). Metamorphic Rocks. A Classification and Glossary of Terms. Cambridge, Cambridge University Press, 244pp.

Dalla Salda, L., 1981. Tandilia, un ejemplo de tectónica de transcurrencia en basamento. Revista de la Asociación Geológica Argentina, 43(2), 198-209.

Dalla Salda, L., Bossi, J., Cingolani, C., 1988. The Río de la Plata cratonic region of southwestern Gondwanaland. Episodes, 11(4), 263-269.

Di Toro, G., Pennacchioni, G., 2004. Superheated friction-induced melts in zoned pseudotachylytes within the Adamello tonalites (Italian Southern Alps). Journal of Structural Geology, 26(10), 1783-1801.

Di Toro, G., Pennacchioni, G., Nielsen, S., 2009. Pseudotachylytes and earthquake source mechanics. In: Fukuyama, E. (ed.). Fault-Zone Properties and Earthquake Rupture Dynamics. Elsevier Academic Press, 87-133.

Fabbri, O., Lin, A., Tokushige, H., 2000. Coeval formation of cataclasite and pseudotachylyte in a Miocene forearc granodiorite, southern Kyushu, Japan. Journal of Structural Geology, 22, 1015-1025.

Frisicale, M.C., Dimieri, L.V., Dristas, J.A., 1998. The Boca de la Sierra megashear zone, Tandilia, Argentina. Terra Nostra. Bayreuth, 16 Geowissenschaftliches Lateinamerika Kolloquium, Abstracts, 39.

Frisicale, M.C., Dimieri, L.V., Dristas, J.A., 2001. Cinemática de las milonitas del basamento en Boca de la Sierra, Sierras de Azul, Buenos Aires. Revista de la Asociación Geológica Argentina, 56(3), 319-330.

Frisicale, M.C., Dimieri, L.V., Dristas, J.A., 2004. Deformación dúctil en el Cerro Negro, megacizalla de Azul, Tandilia, Provincia de Buenos Aires. Asociación Geológica Argentina Serie D, 7, 82-88.

Frisicale, M.C., Martínez, F.J., Dimieri, L.V., Dristas, J.A., 2005. Microstructural analysis and P-T conditions of the Azul megashear zone, Tandilia, Buenos Aires province, Argentina. Journal of South American Earth Sciences, 19, 433-444.

Frisicale, M., Dimieri, L., Dristas, J., 2006. Pseudotaquilitas en la megacizalla de Azul, Tandilia. Asociación Geológica Argentina Serie D, 10, 174-179.

Frisicale, M., Dimieri, L., Araujo, V., Dristas, J., 2010. Mecanismos de deformación en la transición milonitas/*striped gneiss* y milonitas/ultramilonitas en las Sierras de

Azul, cratón del Río de la Plata, Buenos Aires. Revista de la Asociación Geológica Argentina, 67, 4-18.

González Bonorino, F., Zardini, R., Figueroa, M., Limousin, T., 1956. Estudio geológico de las Sierras de Olavarría y Azul (Prov. De Buenos Aires). Lemit, Serie 2, 63, 1-22.

Grant, J.A., 1986. The isocon diagram a simple solution to Gresen´s equation for metasomatic alteration. Economic Geology, 81, 1976-1982.

Hartmann, L.S., Santos, J.O.S., Cingolani, C.A., McNaughton, N.J., 2002. Two Palaeoproterozoic orogenies in the evolution of the Tandilia Belt, Buenos Aires, as evidenced by Zircon U-Pb SHRIMP geochronology. International Geology Review, 44, 528-543.

Iacumin, M., Piccirillo, E.M., Girardi, V.A.V., Teixeira, W., Bellieni, G., Echeveste, H., Fernández, R., Pinese, J.P.P., Ribot, A., 2001. Early Proterozoic calc-alkaline and middle Proterozoic tholeiitic dyke swarms from central-eastern Argentina: petrology, geochemistry, Sr-Nd isotopes and tectonic implications. Journal of Petrology, 42(11), 2109-2143.

Kruse, R., Stünitz, H., 1999. Deformation mechanisms and phase distribution in mafic high-temperature mylonites from the Jotun Nappe, southern Norway. Tectonophysics, 303, 223-249.

Lin, A., 1994. Glassy pseudotachylyte veins from Fuyun fault zone, northwest China. Journal of Structural Geology, 16, 71-83.

Lin, A., Shimamoto, T., 1998. Selective melting processes as inferred from experimentally-generated pseudotachylytes. Journal of Asian Earth Sciences, 16, 533-545.

Lin, A., 1999. Roundness of clasts in pseudotachylytes and cataclastic rocks as an indicator of frictional melting. Journal of Structural Geology, 21, 473-478.

Lin, A., Sun, Z., Yang, Z., 2003. Multiple generations of pseudotachylyte in the brittle to ductile regimes, Qinling-Dabie ultrahigh-pressure metamorphic complex, central China. The Island Arc, 12, 423-435.

Lin, A., Maruyama, T., Aaron, S., Michibayashi, K., Camacho, A., Kano, K., 2005. Propagation of seismic slip from brittle to ductile crust: Evidence from pseudotachylyte of the Woodroffe thrust, central Australia. Tectonophysics, 402, 21-35.

Lin, A., 2008a. Fossil Earthquakes: Formation and Preservation of Pseudotachylytes. Berlin, Springer, 348pp.

Lin, A., 2008b. Seismic slip in the lower crust inferred from granulite-related pseudotachylyte in the Woodroffe thrust, Central Australia. Pure and Applied Geophysics, 165, 215-233.

Maddock, R.H., 1992. Effects of lithology, cataclasis and melting on the composition of fault-generated pseudotachylytes in Lewisian gneiss, Scotland. Tectonophysics, 204, 261-278.

Magloughlin, J.F., 1992. Microstructural and chemical changes associated with cataclasis and frictional melting at shallow crustal levels: the cataclasite-pseudotachylyte connection. Tectonophysics, 204, 243-260.

McKenzie, D., Brune, J.N., 1972. Melting on fault planes during large earthquakes. Geophysical Journal of the Royal Astronomical Society, 29, 65-78.

McNulty, B., 1995. Pseudotachylyte generated in the semi-brittle regimes, Bench Canyon shear zone, central Sierra Nevada. Journal of Structural Geology, 17, 1507-1521.

O'Connor, J.T., 1965. Granite Classification using the Ab-An-Or diagram. In: Rollinson, H.R. (ed.). Using geochemical data: Evaluation, Presentation, Interpretation. Longman, 58-60.

O'Hara, K.D., 1992. Major and trace elements constrains on the petrogenesis of a fault related pseudotachylyte, western Blue Ridge province, North Carolina. Tectonophysics, 204, 270-288.

O'Hara, K.D., Sharp, Z.D., 2001. Chemical and oxygen isotope composition of natural and artificial pseudotachylyte: role of water during frictional fusion. Earth and Planetary Science Letters, 184, 393-406.

Otsuki, K., Hirono, T., Omori, M., Sakaguchi, M., Tanigawa, W., Lin, W., Soh, W., Rong, S., 2009. Analyses of pseudotachylyte from Hole-B of Taiwan Chelungpu Fault Drilling Project (TCDP); their implications for seismic slip behaviors during the 1999 Chi-Chi earthquake. Tectonophysics, 469, 13-24.

Pankhurst, R.J., Ramos, V.A., Linares, E., 2003. Antiquity of the Río de la Plata craton in Tandilia, southern Buenos Aires province, Argentina. Journal of South American Earth Sciences, 16, 5-13.

Passchier, C., Trouw, R., 2005. Microtectonics. Berlin, Springer Verlag, 366pp.

Powell, R., Holland, T.J.B., Worley, B., 1998. Calculating phase diagrams in volving solid solutions via non-linear equations, with examples using Thermocalc. Journal of Metamorphic Geology, 16, 577-588.

Pryer, L., 1993. Microstructures in feldspars from a major crustal thrust zone: the Grenville Front, Notario, Canada. Journal of Structural Geology, 15, 21-36.

Ramos, V.A., 1999. Rasgos estructurales del territorio Argentino. Evolución tectónica de la Argentina. In: Caminos, R. (ed.). Geología Argentina. Buenos Aires, Anales, Servicio Geológico Minero Argentino (SEGEMAR), 29(24), 715-784.

Rapela, C.W., Pankhurst, R.J., Casquet, C., Fanning, C.M., Baldo, E.G., González-Casado, J.M., Galindo, C., Dahlquist, J., 2007. The Río de la Plata craton and the assembly of SW Gondwana. Earth Science Reviews, 83, 49-82.

Reynolds, S.J., Goodwin, L.B., Lister, G.S., Ellzey, P.D., Ferranti, C.J., 1998. Development of ultramylonite from pseudotachylyte in a metamorphic core complex. In: Snoke, A., Tullis, J., Todd, V. (eds.). Fault-related rocks. A photographic Atlas. Princeton University Press, 124-125.

Sibson, R.H., 1975. Generation of pseudotachylyte by ancient seismic faulting. Geophysical Journal of the Royal Astronomical Society, 43, 775-794.

Sibson, R.H., 1980. Transient discontinuities in ductile shear zones. Journal of Structural Geology, 2, 165-171.

Spray, J.G., 1992. A physical basis for the frictional melting of some rock-forming minerals. Tectonophysics, 204, 205-221.

Spray, J.G., 1995. Pseudotachylyte controversy: Fact or friction? Geology, 23, 1119-1122.

Swanson, M.T., 1992. Fault structure, wear mechanisms and rupture processes in pseudotachylyte generation. Tectonophysics, 204, 223-242.

Takagi, H., Goto, K., Shigematsu, N., 2000. Ultramylonite bands derived from cataclasite and pseudotachylyte in granites, northeast Japan. Journal of Structural Geology, 22, 1325-1339.

Teixeira, W., Pinese, J.P.P., Iacumin, M., Girardi, V.A.V., Piccirillo, E.M., Echeveste, H., Ribot, A., Fernández, R., Renne, P.R., Heaman, L.M., 2001. Geochronology of calc-alkaline and tholeiitic dyke swarms of Tandilia, Río de la Plata craton, and their role in the paleoproterozoic tectonics. Pucón (Chile), III South American Symposium of Isotope Geology, Santiago de Chile, Extended abstract, CD-Rom, Servicio Nacional de Geología y Minería (SENARGEO-MIN), 257-260.

Teruggi, M.E., Kilmurray, J.O., Dalla Salda, L., 1973. Los dominios tectónicos de la región de Tandil. Anales Sociedad Científica Argentina, 95(1-2), 81-96.

Teruggi, M., Kilmurray, J., Dalla Salda, L., 1974. Los dominios tectónicos de la región de Balcarce. Revista de la Asociación Geológica Argentina, 29(3), 265-276.

Thompson, L.M., Spray, J.G., 1996. Pseudotachylyte petrogenesis: constraints from the Sudbury impact structure. Contributions to Mineralogy and Petrology, 125(4), 359-374.

Trouw, R.A.J., Passchier, C.W., Wiersma, D.J., 2010. Atlas of mylonites and related microstructures. Berlin, Springer Verlag, 322pp.

Warr, L.N., van der Pluijm, B.A., Peacor, S.R., Hall, S.M., 2003. Frictional melt pulses during a ~1.1Ma earthquake along the Alpine Fault, New Zealand. Earth and Planetary Science Letters, 209, 39-52.

Wenk, H.R., Jonson, L.R., Ratschbacher, L., 2000. Pseudotachylytes in the Eastern Peninsular Ranges of California. Tectonophysics, 321, 253-277.

Wenk, H.R., Weiss, L.E., 1982. Al-rich calcic pyroxene in pseudotachylyte: an indicator of high pressure and high temperature? Tectonophysics, 84, 329-341.

Manuscript received December 2009;
revision accepted March 2011;
published Online September 2011.